Journal of Materials Chemistry A

PAPER

View Article Online
View Journal | View Issue

Cite this: J. Mater. Chem. A, 2014, 2, 9792

Use of a new crosslinking method to obtain semi-IPN membranes with phosphonic acid groups for a PEMFC application†

Etienne Labalme,[a] Ghislain David,*[a] Julien Souquet,[b] Pierrick Buvat[b] and Janick Bigarre[b]

Received 27th March 2014
Accepted 24th April 2014

DOI: 10.1039/c4ta01472c

www.rsc.org/MaterialsA

The synthesis of a new semi-IPN membrane was performed from a commercial fluorinated copolymer and a fluorophosphonated copolymer with pendant phosphonic acid groups. The crosslinking of the fluorophosphonated copolymer was done from the presence of sulfonated groups by a simple heat treatment. Several membranes are cast with a crosslinking rate range from 5 to 20% and a molar percent of phosphonic acid range from 38 to 12%. These kinds of PEMFCs show proton conductivity in a reach magnitude of 10^{-3} S cm^{-1} in humidified conditions. All the membranes possess a high thermal stability. The mechanical behaviour of all membranes was determined by DMA as a function of the temperature and the relative humidity.

Introduction

During recent years, many research works have been carried out on new-technology development in order to use fuel cells as a new energy source. One of the main subjects of research was the amelioration of the proton exchange membrane performance, which is the heart of the fuel cell. Nowadays, the most used membranes are perfluorosulfonic polymers (Nafion®, Aquavion®…), which allow the best performances to be reached in a moderate range of temperatures between 25 and 80 °C and a high level of hydration with a required high relative humidity (more than 50% RH).

Nevertheless, in the automotive sector, fuel cell specifications were defined to be used nominally at 120 °C with 30% RH and a low pressure. Under these conditions, perfluorosulfonic membrane performances fall drastically due to the loss of water. This implies the necessity to develop membranes with novel protogenic groups able to give proton conduction in low hydration conditions and at 120 °C. In these conditions, membranes bearing phosphonic acid groups seem to be good potential candidates.[1,2] Indeed, the proton conductivity of phosphonic acid polyelectrolytes was better than sulfonated polymer at elevated temperatures and in a dry state. This higher proton conductivity demonstrates the amphoteric character of the acid phosphonic groups associated with a proton transport by a Gröthuss mechanism.[3] Furthermore, phosphonic acid-functionalized polyelectrolytes permit material with low water swelling to be obtained, which improves the mechanical stability during cycle of use. Then, during recent years different works were carried out on the synthesis of different polyarylphosphonic acid functionalized[4–9] or polystyrene derivatives carrying phosphonic acid groups.[10,11]

Previous works performed by our team[12–14] involved the synthesis of partially fluorinated copolymer bearing phosphonic acid groups. Thanks to the acceptor/donor character of monomers used for the polymerization, the polymer obtained showed an alternated structure[15] between fluorinated and phosphonic acid units, which allows the presence of phosphonic acid groups distributed along the polymer. Interestingly, this polymer was used as a PEMFC and showed a very good thermal stability (up to 200 °C). Furthermore, when decreasing RH from 95 to 25%, the conductivity values decrease only 1 order of magnitude, while the Nafion® conductivity drop about 3 orders of magnitude in the same range. Furthermore, an increase of the temperature (from 90 to 120 °C) leads to an increase of the proton conductivity by two in the same range of RH. However, the molar mass of the polymer obtained was about 20 000 g mol^{-1}; this implies that resulting membranes exhibit very poor mechanical properties, as they were very brittle. These low mechanical properties greatly limit their use in dry conditions, as well as decrease the life time of the membrane.

So, in order to improve the mechanical properties of the PEMFC a blend strategy was used.[16] To do this, the copolymer carrying phosphonic group (under the ester phosphonate form) was blended with a highly fluorinated copolymer. Indeed, polymer blending is gaining ground as a promising

[a]Equipe Ingénierie et Architecture Macromoléculaires, Institut Charles Gerhardt UMR CNRS 5253, Ecole Nationale Supérieure de Chimie de Montpellier, 8 rue de l'Ecole Normale, 34296 Montpellier Cedex 5, France. E-mail: ghislain.david@enscm.fr

[b]CEA, DAM, Le Ripault, F-37260 Monts, France

† Electronic supplementary information (ESI) available. See DOI: 10.1039/c4ta01472c

methodology for the development of PEMs. Nevertheless, during the acidification reaction of the phosphonate groups, membrane breakdowns were observed. Indeed, the conditions of the acidification reaction are drastic (hydrochloric acid solution concentrated at 12 N, at a temperature of 90 °C for 3 days). Furthermore, the strong hydrophilic/hydrophobic balance between the two polymers resulted in only partial miscibility. In order to use all the potential of these kinds of membranes, an improvement in two crucial points (*i.e.* the acid degradation and the partial miscibility) is required. In order to solve these problems, the most suitable method consists of crosslinking the phosphonated copolymer. However, the conditions of PEMFC are quite extreme; high concentration of acid, high temperature, and presence of radicals. It is thus necessary to perform the crosslinking through the formation of strong covalent bonding that will enable the membrane to resist this hostile environment. In this framework, the formation of ether bonds between the polymer chains appears to realize all these requirements. The objective of this work is to develop a strategy to achieve crosslinking through thermal activation without the addition of catalyst or initiator.

In this work we evaluate the feasibility of semi-interpenetrated networks (SIPN) obtained by blending poly(VDF-*co*-CTFE) (inert matrix, mechanical support phase) with covalently crosslinked phosphonated polyelectrolytes (proton conducting phase) as potential PEM material candidates. To perform the crosslink of the phosphonated copolymer a new chemical method based on the sulfonated groups will be used.[17] So, the first part of this work is concentrated on the feasibility of the crosslinking reaction. Then, thermal and mechanical properties are examined for a wide range of membranes. Especially, the impact of the crosslinking ratio on the membranes' properties is studied. The proton conductivity of membranes that possess the higher IECs was assessed.

Results and discussion

Study of crosslinking reaction

The crosslinking technique is based on the reactivity mesylate functional groups, allowed to crosslink the copolymer *via* interchain ether bonds. To do this, we relied on the work of Sach *et al.*[18] who performed the synthesis of aryl ethers from primary and secondary alcohols and aryl mesylates. The reaction proceeds *via* a sulfonyl transfer mechanism. A proposed mechanism of this reaction is shown in Scheme 1. The first step of this mechanism is the formation of the sulfene *via* an E2 elimination of the alcoholate. This reaction is thermally promoted, so at high temperatures, the sulfene formation can be expected without the presence of based.

To demonstrate the validity of the crosslinking reaction described above, a model copolymer was synthesized from the polymerization of CTFE and ethyl vinyl ether (EVE) and 4-(vinyloxy)butyl methanesulfonate (VBMS) (Scheme 2). The synthetic route for VBMS (2) is shown in Scheme 2. Monomer 2 was easily synthesized from 4-(vinyloxy)butan-1-ol (monomer 1) and methanesulfonyl chloride by a Williamson reaction with high yield. The structure of monomer 2 was confirmed by ^{1}H NMR (ESI†).

The copolymer synthesis is performed by radical terpolymerization between chlorotrifluoroethylene (CTFE), ethyl vinyl ether (EVE) and VBMS, as indicated in Scheme 3 (where "*x*" is the molar percentage of VBMS in the feed).

The model study will be conducted without a phosphonated group on the terpolymer, *i.e.* without using DEVEP. Indeed, the presence of this group could influence the crosslinking mechanism. To limit the amount of monomer carrying the reactive function, the synthesis will be carried out from a mixture of CTFE, ethyl vinyl ether (EVE) and VBMS in the molar proportions 50/45/5, respectively.

The copolymer obtained, *i.e.* the poly[(CTFE-*alt*-EVE)$_{0.9}$-*co*-(CTFE-*alt*-VBMS)$_{0.1}$], was characterized by ^{1}H NMR (Fig. 1) to confirm the good incorporation of VBMS in the polymer chain. Based on the previous works[15] carried out on the alternated copolymerization of chlorotrifluoroethylene with vinyl ethers, various significant signals of the methyl and methylene groups were clearly identified. The presence of groups signals:

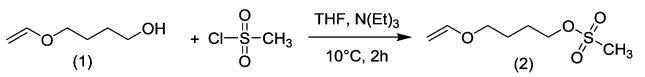

Scheme 2 Synthesis of 4-(vinyloxy)butyl methanesulfonate (VBMS).

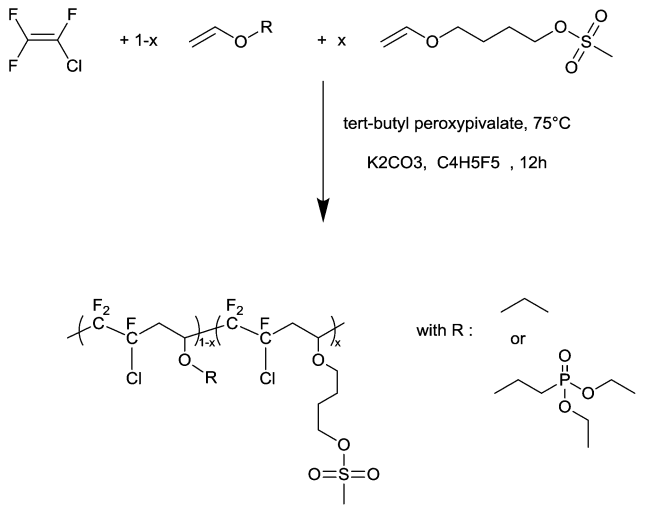

Scheme 3 Radical terpolymerizations.

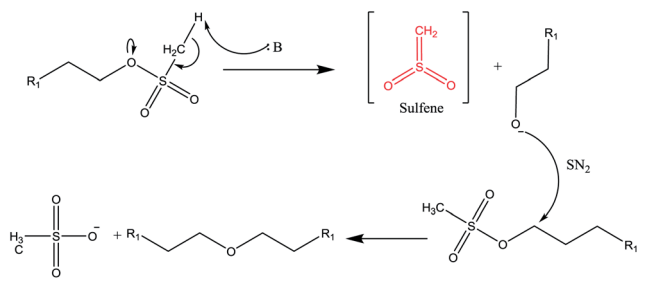

Scheme 1 Synthesis of ether bond from the sulfonate groups.[18]

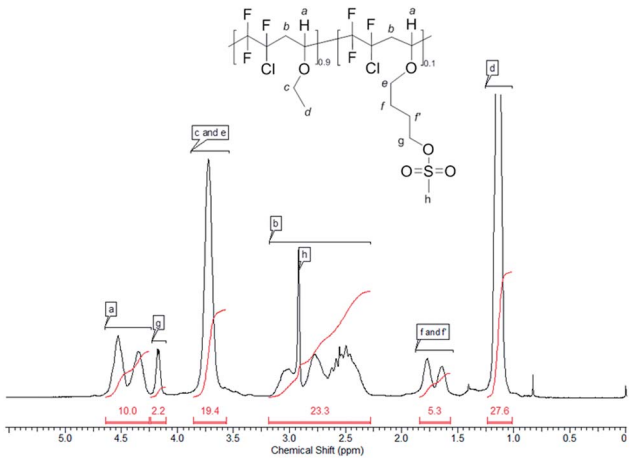

Fig. 1 ^{1}H NMR spectrum of poly(CTFE-*alt*-EVE)$_{0.9}$-*co*-(CTFE-*alt*-VBMS)$_{0.1}$ performed in $CDCl_3$.

–O–CH_2–CH_2–CH_2–CH_2–O–S(O)$_2$–CH_3 (*e*), –O–CH_2–CH_2–CH_2–CH_2–O–S(O)$_2$–CH_3 (f, f′), –O–CH_2–CH_2–CH_2–CH_2–O–S(O)$_2$–CH_3 (*g*); –O–CH_2–CH_2–CH_2–CH_2–O–S(O)$_2$–CH_3 (h), respectively, centred at 3.79, 1.71, 1.84, 4.25 and 3.02 ppm allows confirmation of the incorporation of VBMS in the terpolymer chain. The ^{19}F NMR spectrum of the product, available in the ESI,† allows confirmation of the alternated character of the copolymer.

In order to determine the efficiency of the crosslinking reaction, different analyses have been performed on the membrane before and after the crosslinking reaction. To perform the cross-linking reaction, the terpolymer solution was cast onto a glass plate, and then dried at 80 °C for 12 h to eliminate the solvent and obtain the uncrosslinked membrane, and then at 150 °C to perform the crosslink reaction to obtain the resulting membrane.

Thermal analyses

The thermal stability of the membrane has been assessed by thermogravimetric analysis (TGA) before and after the crosslinking reaction. Fig. 2 shows the thermogram obtained by TGA analyses of the membrane cast from the poly[(CTFE-*alt*-EVE)$_{0.9}$-*co*-(CTFE-*alt*-VBMS)$_{0.1}$] before (–) and after (–) crosslinking. The derivative curves are also given.

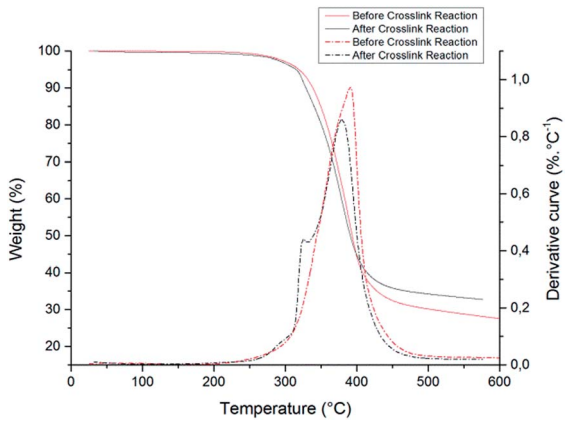

Fig. 2 TGA analyses of poly[(CTFE-*alt*-EVE)$_{0.9}$-*co*-(CTFE-*alt*-VBMS)$_{0.1}$] before and after the crosslinking reaction.

Before crosslinking, we can note two main decompositions between 270 and 500 °C. The first degradation occurs between 270 and 330 °C. The bond energy dissociation (–O–S) of C–O–S(O_2)–CH_3 groups is weaker than the bond energy (–O–C) of –C–O–CH_2CH_3 groups, so we can attribute this weight loss to the dissociation of the –O–S– bond of VBMS units. Then from 350 °C, the degradation of all the pendant polymer chains can be observed. After crosslinking, only one decomposition was observed in the range from 270 to 500 °C. Indeed, between 270 and 330 °C on the derivative curve, the peak attributed to the –O–S– bond dissociation of VBMS units is no longer observed. Thus, during the crosslinking reaction, it seems that all mesylate groups are consumed. We also note that the crosslinked membrane has a slightly higher thermal stability than the non-crosslinked membrane. This increase of the thermal stability resulted in a slight increase of both $Td_{5\%}$ and $Td_{10\%}$ (Table 1). Indeed, after crosslinking, the temperature corresponding to a 10% weight loss ($Td_{10\%}$) is 338 °C, whereas for the non-crosslinked membrane, the $Td_{10\%}$ is 328 °C.

The glass transition temperatures of the terpolymers before and after crosslinking reactions were determined by DSC. The results obtained are listed in Table 1. The T_g value is 10 °C before crosslinking, and increases to reach 90 °C after crosslinking. This increase in the glass transition temperature characterizes a significant polymer network rigidification due to the formation of inter-chain bridges during the second heat treatment at 150 °C.

Terpolymer solubility

The crosslinking reaction of the terpolymer leads to a three-dimensional network due to the formation of inter-chain bonds. This will directly impact the solubility of the polymer in various organic solvents, even resulting in total insolubility of the polymer for a sufficient degree of crosslinking. Thus, in order to confirm the crosslinking of membranes, solubility tests were carried out in different solvents. The test consists of immersing the membrane in the solvent for a period of 72 hours with weak stirring. The tests were conducted at both room temperature and 50 °C (Table 2).

Table 1 Degradation temperatures and glass transition temperatures of poly[(CTFE-*alt*-EVE)$_{0.9}$-*co*-(CTFE-*alt*-VBMS)$_{0.1}$] before and after crosslinking obtained, respectively, by TGA under nitrogen at 20 °C min^{-1} and DSC at 20 °C min^{-1}

Membranes	$Td_{5\%}$ (°C)	$Td_{10\%}$ (°C)	T_g[a] (°C)
Before crosslinking	314	328	10
After crosslinking	319	338	90

[a] Uncertainty for the glass transition temperature determined by DSC: ±2 °C.

Table 2 Solubility tests at RT and 50 °C of poly[(CTFE-*alt*-EVE)$_{0.9}$-*co*-(CTFE-*alt*-VBMS)$_{0.1}$] before and after crosslinking

		After crosslinking	
Solvent	Before crosslinking	T = RT	T = 50 °C
Methanol	+[a]	×[b]	×
Acetone	+	×	×
MEK	+	×	×
THF	+	×	×
DMSO	+	×	×
DMF	+	×	×

[a] + = soluble. [b] × = insoluble.

From Table 2, we note that the thermal treatment allows membranes to become totally insoluble in most organic solvents after crosslinking, at room temperature but also at 50 °C. The insolubility of the membranes, especially in the solvents used for the casting, confirms the success of the crosslinking reaction of the membrane during heat treatment.

FTIR analyses

Fourier transform infrared spectroscopy (FTIR) analyses have been performed on terpolymer before and after the crosslinking reaction (Fig. 3). From FTIR, the sulfonate groups are characterized by the presence of two bands around 1150 and 1350 cm^{-1}. Although the TGA results show a total consumption of mesylate groups after heat treatment, we observe a slight decrease of the characteristic band. But, the band characteristic of ether bonds significantly increases. The emergence of a new band between 1700 and 1800 cm^{-1} can be observed. This band is characteristic of carbonyl bonds. In view of the required thermal crosslinking of the terpolymer (>150 °C), this band cannot be characteristic of the formation of ester or aldehyde groups. This band probably corresponds to the formation of a ketone group during the crosslinking reaction. Further investigations are, nevertheless, necessary to fully understand this reaction.

The crosslinking reaction probably occurs *via* the formation of ether and ketone bonds. During the reaction, the denser polymer network thereby reduces the mobility of the remaining sulfonate groups. In addition, we did not find any mechanism that could explain the formation of ketone groups. A model study from the coupling molecule with a mesylate or tosylate group will be carried out to obtain more insight about the reaction occurring during the crosslinking of the copolymer.

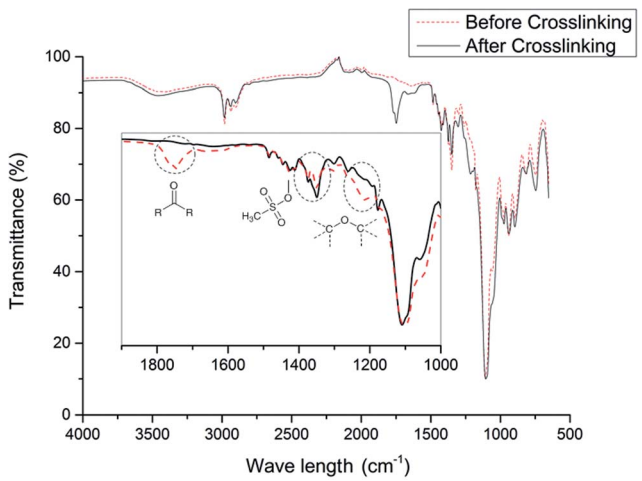

Fig. 3 FTIR spectrum of poly[(CTFE-*alt*-EVE)$_{0.9}$-*co*-(CTFE-*alt*-VBMS)$_{0.1}$] before and after crosslinking.

Preparation of semi-IPN membranes

The copolymer synthesis was performed by radical terpolymerization between chlorotrifluoroethylene (CTFE), diethyl vinyl ether phosphonated (DEVEP) and VBMS as indicated in Scheme 3. The structure of poly[(CTFE-*alt*-DEVEP)$_{1-x}$-*co*-(CTFE-*alt*-VBMS)$_x$] was confirmed by ^{1}H NMR, as shown in Fig. 4. The integral ratio of signals between 1.6 and 1.9 ppm (H_h) and between 4.35 and 4.75 ppm (H_a) was calculated to confirm that the terpolymer composition corresponds to the initial stoichiometric proportion. In order to study the effect of the crosslink density on physico-chemical properties of the membranes, we have synthesized the fluorophosphonate terpolymer with VBMS contents of 5, 10 and 20 mol%, respectively P_5, P_{10} and P_{20}. The molar content of VBMS, DEVEP and CTFE is ascribed in Table 3 for each terpolymer.

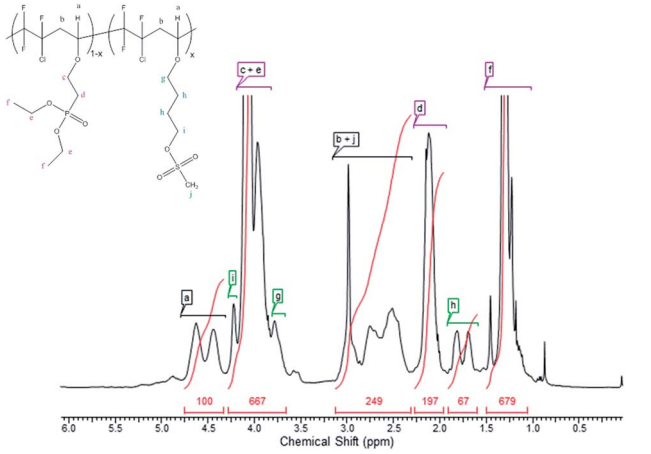

Fig. 4 ^{1}H NMR spectrum of poly[(CTFE-*alt*-DEVEP)-*co*-(CTFE-*alt*-VBMS)] (realized in $CDCl_3$).

Table 3 Terpolymers composition

	Molar ratio of monomers into the terpolymer[a] (%)		
Terpolymers	CTFE	DEVEP	VBMS
P_5	50	43	7
P_{10}	50	39	11
P_{20}	50	31	19

[a] Determined by ^{1}H NMR.

The membranes were prepared from film casting of a polymeric solution of poly(VDF-*co*-CTFE) and poly[(CTFE-*alt*-DEVEP)$_{1-x}$-*co*-(CTFE-*alt*-VBMS)$_x$] (Fig. 5). After the evaporation of the cast solvent, membranes were heated at 150 °C to perform the crosslinking reaction. Cleavage of the ester groups from the phosphonate was then performed in 12 N HCl solution at 90 °C for 3 days. No coloration was observed during the acidification process, which proves that crosslinking allows the polymer stabilization. Indeed, in the previous work,[16] the acidification of the poly(CTFE-*alt*-DEVEP) by the same method resulted in a coloration of the acid solution. From the three synthesized terpolymers, a range of membranes was synthesized by varying the content of poly(VDF-*co*-CTFE). The membranes have been noted M$_x$-*Y*, where *x* is the molar content of VBMS in the copolymer and *Y* is the mass content of poly[(CTFE-*alt*-DEVEP)-*co*-(CTFE-*alt*-VBMS)]. For instance M$_5$-80 was obtained from 80 wt% of poly[(CTFE-*alt*-DEVEP)-*co*-(CTFE-*alt*-VBMS)], which contains 5 mol% of VBMS. The different membranes performed for this study are gathered in Table 4. The minimum rate of fluorophosphonate terpolymer was 30 wt% in order to get sufficient values of IECs into the semi-IPN membranes. Moreover, the minimum rate of poly(VDF-*co*-CTFE) was assessed to be 20 wt% to afford sufficient mechanical properties for fuel cell applications.

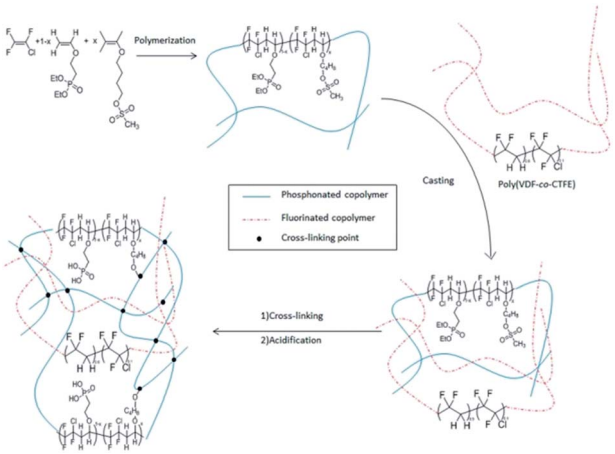

Fig. 5 Schematic representation of procedure to obtain pseudo semi-IPN membrane comprising crosslinked poly[(CTFE-*alt*-DEVEP)-*co*-(CTFE-*alt*-VBMS)] and poly(VDF-*co*-CTFE).

Thermal properties of the membranes

The thermal properties of the different membranes were assessed after the crosslinking reaction and acidification step. The temperatures corresponding to weight losses of 5 and 10% (respectively Td$_{5\%}$ and Td$_{10\%}$) and the glass transition temperature (T_g) values for all the membranes are gathered in Table 4 (respectively determined by ATG and DSC). For all the membranes, the Td$_{5\%}$ is highest at 250 °C. So, the thermal stability of this kind of membrane is clearly sufficient for PEMFC applications.

The glass transition temperatures were determined for each membrane before and after acidification. The T_g values clearly increase for all membranes after the acidification reaction, which proves that the phosphonic acid groups undergo hydrogen bonding between them. Thus more energy is then required to go from the viscous to the glassy state. In Fig. 6, we have plotted the evolution of the T_g values *vs.* the content of fluorophosphonate terpolymer for the membranes M$_5$, M$_{10}$ and M$_{20}$ after acidification.

For membranes M$_5$, M$_{10}$ and M$_{20}$, T_g values increase with a decrease of the fluorophosphonate terpolymer content until reaching a maximum for 50% of terpolymer; below this content the T_g values slightly decrease. The decrease of fluorophosphonate terpolymer content to 80 °C at 50%, in the membranes probably allows the phosphonic acid groups to be closer to each other and so to an increase in the hydrogen bonding.[16] But when the content of fluorophosphonate terpolymer becomes too low, *i.e.* 30 wt%, this effect is no longer predominant and thus the T_g values decrease. Finally, we can

Table 4 Composition, degradation temperatures at 5 and 10% weight loss, glass transition temperature and theoretical and experimental IEC of the all semi-IPN membranes obtained, respectively, by TGA in dynamic mode at 20 °C min^{-1} and obtained from DSC at 20 °C min^{-1}, and by acido–basic titration

Membranes	Rate of fluorophosphonate terpolymer (wt%)	Rate of poly(VDF-*co*-CTFE) (wt%)	Rate of phosphonic acid (mol%)	Td$_{5\%}$ (°C)	Td$_{10\%}$ (°C)	$T_g{}^d$ (°C)	$T_g{}^e$ (°C)	IEC$_{theo}$ (meq. g^{-1})	IEC$_{exp}$ (meq. g^{-1})
M$_5$-80[a]	80	20	38	285	310	11	92	5.32	2.1
M$_5$-60[a]	60	40	28.5	295	318	10.5	95.5	3.99	0.44
M$_5$-50[a]	50	50	23.75	287	304	12	108	3.15	0.8
M$_5$-30[a]	30	70	14.25	316	333	−5	85.8	2	0.4
M$_{10}$-80[b]	80	20	36	283	308	31	92.5	5.04	1
M$_{10}$-60[b]	60	40	27	286	311	54	98	3.78	0.3
M$_{10}$-50[b]	50	50	22.5	288	313	55	105	3.15	0.4
M$_{10}$-30[b]	30	70	13.5	310	330	1	101.4	1.89	0.52
M$_{20}$-80[c]	80	20	32	284	305	54	92	4.48	0.9
M$_{20}$-60[c]	60	40	24	295	314	90	98	3.36	0.5
M$_{20}$-50[c]	50	50	20	300	322	80	115	2.8	0.8
M$_{20}$-30[c]	30	70	12	311	334	76	90.8	1.68	0.9

[a] Terpolymer P$_5$. [b] Terpolymer P$_{10}$. [c] Terpolymer P$_{20}$. [d] Before acidification reaction. [e] After acidification reaction.

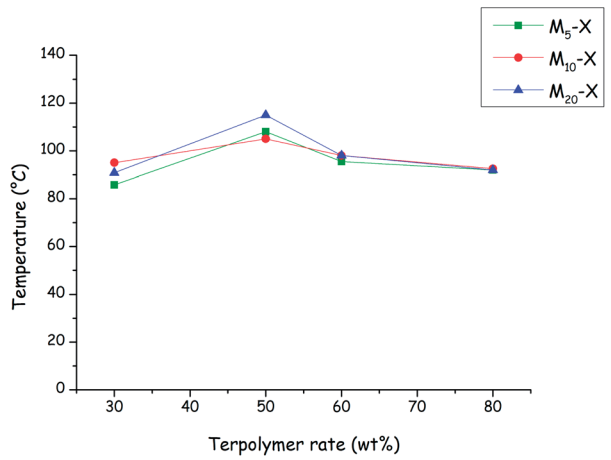

Fig. 6 Evolution of T_g *vs.* the content of fluorophosphonate terpolymer for the membranes M_5, M_{10} and M_{20} after acidification.

note that the content of cross-linking agent does not really impact the T_g values of the membranes.

Water uptake and swelling ratio

Water uptake of the membranes is a key parameter for the electro-chemical performances of the PEMFC as well as for the mechanical properties. Indeed, water is essential for the proton transport through a vehicular mechanism. Even if membranes made from fluorophosphonate polymers are to be used at high temperatures (from 90 to 130 °C) and at low relative humidity (RH < 50%), these membranes have to show sufficient water uptake to undergo proton transport at a low temperature and high RH as well. Nevertheless, too high a water uptake will therefore lead to a sharp decrease of the mechanical properties of the membrane during the fuel cell operation. We have determined the water uptake for all the membranes at room temperature and at 100% RH (Fig. 7).

The experimental water uptakes (WUs) were compared to the theoretical ones, calculated from the WUs of poly(CTFE-*alt*-VEPA), to be about 65% at 100% RH and room temperature[14] (Fig. 7). Concerning first the M_5 membranes, both experimental and theoretical WU values are very close, which means that all the phosphonic acid groups are easily accessible in the membrane. But, when the membranes are more densely crosslinked, *i.e.* M_{10} and M_{20} membranes, the accessibility to the phosphonic acid groups remains limited; this is the reason why we note a discrepancy between the experimental and theoretical WU values for M_{10} and M_{20} membranes. We can remark that both M_{10}-80 and M_{10}-60 show a WU of about 20%, which should be enough to reach good proton conductivity. For M_{20}-*X* membranes, the WU remains lower than 10%, which seems to be detrimental to proton conductivity.

The swelling rate of the membranes is also a key parameter to take into account for PEMFC use. The swelling is characterized by an increase of the membrane thickness due to water uptake. During the fuel cell operation, cycles of swelling/unswelling of the membrane are observed. If the membrane swelling is too high, a loss of the mechanical properties occurs during these cycles. Fig. 8 shows the evolution of the swelling rate for the M_5-*X*, M_{10}-*X* and M_{20}-*X* membranes *vs.* the content of fluorophosphonate terpolymer.

We can observe that the swelling rate of the M_{20} membranes is very low, which could be linked to the low water uptake for these membranes. Furthermore, even for a lower content of VBMS, *i.e.* lower crosslinking rate, the swelling rate remains lower than 30%. The crosslinking reaction of the terpolymer in the membrane leads to a network stiffness, which limits the polymer expansion due to the water uptake. The swelling rates showed in Fig. 8 are, nevertheless, acceptable and in the same order as that of Nafion112®.[19] Thus, we expect that the swelling cycles during the fuel cell operation should not lead to a loss of the mechanical properties of the membranes.

Evaluation of the ionic exchange capacity (IEC)

Since poly(CTFE-*alt*-VEPA) shows an alternated structure, the IEC is rather high. Thus the IEC_{theo} values in the case of pseudo semi-IPN membranes are expected to be high. The values are

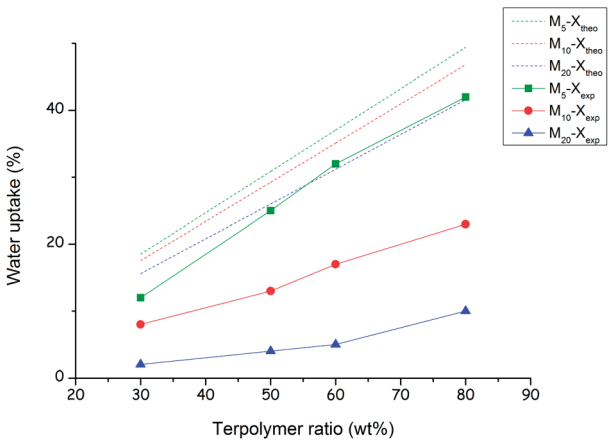

Fig. 7 Evolution of the water uptake *vs.* the content of fluorophosphonate terpolymer for the M_5-*X*, M_{10}-*X* and M_{20}-*X* membranes.

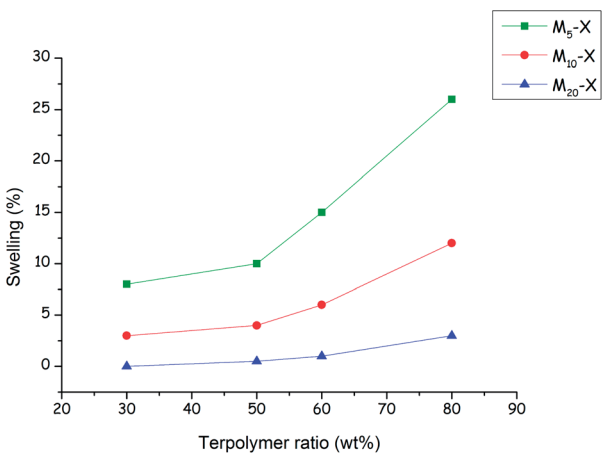

Fig. 8 Evolution of the swelling rate (%) *vs.* the content of fluorophosphonate terpolymer for the M_5, M_{10} and M_{20} membranes.

gathered in Table 4 and range from 5.32 for M_5-80 membrane to 1.68 for M_{20}-30 membrane.

We can see in Table 4 that the IEC_{theo} values are much lower than the IEC_{exp} values. As a reminder, the principle of this method is based on the transformation of phosphonic acid of the membranes in a sodium phosphonate groups. In order to realize the transformation of the phosphonic acid functions from phosphonate groups, it is necessary that the Na^+ cations migrate through the membrane. However, the membrane crosslinking results in an increase of the density of the polymer network, and therefore the accessibility of phosphonic acid groups is much reduced. Indeed, we have already observed that the water uptake values for membranes M_{10}-*X* and M_{20}-*X* are below the theoretical values, so that the phosphonic acid groups are much less accessible. On the other hand, the experimental M_5-*X* water uptake values are in the same order of magnitude as the theoretical values. But, the IEC_{exp} values concerning the M_5-*X* membranes remain lower than the IEC_{theo}. In this case, the polymer network densification allows the migration of water molecule to create a hydration sphere around the phosphonic groups, but for the Na^+ cation the access of the phosphonic acid groups is more difficult, in particular when the solvation effect is considered. However, proton, being much smaller than the cation Na^+, transport through the membrane should be achievable. The measurement of the membrane proton conductivity will allow confirmation of this assumption.

Proton conductivity

The performance of a membrane for PEMFC is closely dependent on the proton conductivity, which directly influences the ohmic losses and finally the power densities. Proton conductivity measurements of M_5-80, M_{10}-80 and M_{20}-80 membranes were performed from 20 to 90 °C in water-immersed conditions in order to characterize the fully hydrated membrane properties (Fig. 9). These results were compared to those of previous work, obtained for the M-100 membrane (cast only from phosphonate terpolymer).[14] These membranes have been chosen because they show the best results due to their higher phosphonated terpolymer rate.

Firstly, the evolution of the proton conductivity *versus* temperature is very different between the M-100 membrane and the M_5-80, M_{10}-80 and M_{20}-80 membranes. Indeed, concerning the M-100 membrane, a decrease of the proton conductivity *versus* temperature is observed. At 20 °C, proton conductivity is around 20 mS cm^{-1} and at 80 °C it is around 1 mS cm^{-1}. In the previous works,[13,14] a diminution of the swelling was demonstrated when the temperature increased, which may explain this behaviour. Concerning the crosslinked membranes, an increase of the proton conductivity *versus* temperature was observed. In this case, the increase of the proton conductivity can be linked to a better structural condition of the membranes. However, the performances of the crosslinked membranes are lower than those of blend membranes.[16] Indeed, the mobility of phosphonic groups was decreased by the crosslinking reaction. So, the macroscopic organization of the crosslinked membrane is not the same as that of the blend membrane. This decrease of proton conductivity can also be attributed to the decrease in phosphonic acid accessibility, due to the higher crosslinking rate.

Mechanical properties

Dynamic mechanical analysis (DMA) was used to study the mechanical properties of the membranes and, in this way, assess the contribution of poly(VDF-*co*-CTFE) on the mechanical properties of blend semi-IPN membranes. Before performing the mechanical study of different semi-IPN membranes, it is necessary to look at the mechanical properties of poly(VDF-*co*-CTFE). For this, the M-0 membrane (cast from only poly(VDF-*co*-CTFE)) was analysed by DMA. The result is shown in Fig. 10.

The variation of storage modulus (E') for a temperature range from −50 to 150 °C is shown Fig. 10. We observe that the storage modulus of the membrane cast only from poly(VDF-*co*-CTFE) is high throughout the temperature range studied. Indeed, it is 2.5 × 10^9 Pa at a temperature of −50 °C, and then decreases steadily to 2.2 × 10^8 Pa at a temperature of 120 °C. Around 70 °C, we observe a slight decrease followed by an increase of the storage modulus. This variation of the modulus corresponds to a

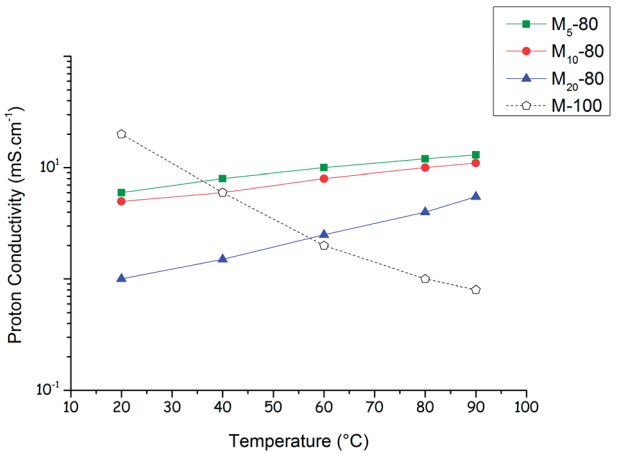

Fig. 9 Average conductivity *versus* temperature in immersed conditions for the M100, M_5-80, M_{10}-80 and M_{20}-80 membranes.

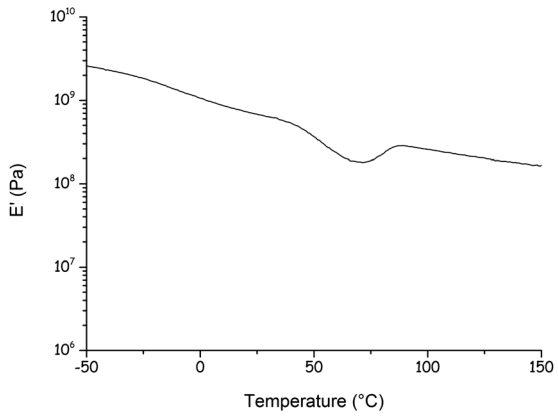

Fig. 10 Storage modulus *versus* temperature of M-0 performed at 1 Hz and 2 °C min^{-1}.

change of the crystallographic state of poly(VDF-*co*-CTFE). Although the T_g of the polymer is −30 °C (determined by DSC), we do not see a drastic drop in the storage modulus; this is due to the semi-crystalline nature of poly(VDF-*co*-CTFE). This semi-crystalline character will bring stability throughout the temperature range used. On the other hand, the DMA analysis of the M-100 membrane (*i.e.* cast only from the poly(CTFE-*alt*-DEVEP) without crosslinking agent) is impossible, since the membrane is too brittle.

Semi-IPN membranes were then analysed by DMA. Two parameters may vary during the analysis: temperature and relative humidity of the measuring chamber. The mechanical behaviour of membranes was measured at temperatures ranging from −50 to 150 °C.

The evolution of the storage modulus for the M_{10}-30, M_{10}-50, M_{10}-60 and M_{10}-80 for a temperature range from 25 to 150 °C is shown Fig. 11. At low temperatures (<0 °C) (Table 5), the mechanical behaviour is the same as that of M-0 membrane (cast only from poly(VDF-*co*-CTFE)). Then, the storage modulus gradually decreases with temperature. From 80 °C, we observed that the storage modulus starts to decrease more significantly, reaching a plateau of 5×10^7 Pa. Indeed, for $T > T_g$, the storage modulus of an amorphous polymer drastically drops, reaching several decades. In our case, the drop of the storage modulus is limited by the presence of poly(VDF-*co*-CTFE) which possesses a storage modulus of about 2×10^8 Pa at this temperature. However, we note that there are slight differences according to the rate of phosphonated polymer. Indeed, for the membrane M_{10}-80, which has the highest rate of phosphonated polymer, the storage modulus is slightly higher, especially for temperatures above 50 °C. However, for $T > T_g$ (T_g of the phosphonated copolymer), the M_{10}-80 membrane shows the lowest modulus values. In contrast, the M_{10}-30 membrane, which has the lowest rate of phosphonated copolymer, for $T < T_g$, has the lowest storage modulus, and for $T > T_g$ it has the highest modulus values. From the curves in Fig. 11, we can determine an approximation of the T_g values of the phosphonated copolymer. To do this, we consider the temperature where the storage modulus starts to sharply decrease. Results are listed in Table 5, where we can see that the T_g values obtained by DMA are similar to that determined by DSC. However, for the membrane M_{10}-30, the influence of the phosphonated copolymer on the mechanical properties is too low to perform the determination of T_g from DMA. From the observation of tan δ, we can see the presence of one maximum around 120 °C (except for the M_{10}-30 membrane). The presence of this maximum signifies a change in the mechanical behaviour of the membranes. However, the mechanical stability was ensured by the presence of the fluorinated copolymer.

From Fig. 12, we can observe that for a temperature of −50 °C the composition of membranes has little influence on the values of the storage modulus. At this temperature, the mechanical properties are dominated by the poly(CTFE-*co*-VDF). However, at temperatures above the T_g of poly(VDF-*co*-CTFE) some variations are observed. For a temperature of 25 °C, the membranes with the highest rate of phosphonated terpolymer (M_5-80, M_{10}-80 and M_{20}-80) show the highest storage modulus values. This behaviour is due to the rigidity of the phosphonated copolymer when the temperature is below its T_g. And for a temperature of 150 °C, we observe the opposite behaviour, *i.e.*, the lowest storage modulus corresponds to

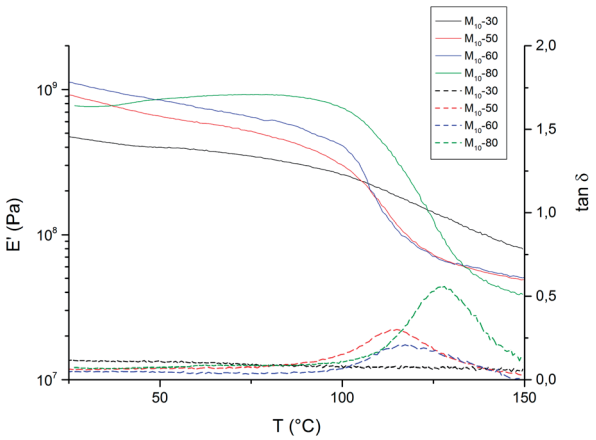

Fig. 11 Storage modulus (—) and tan δ (- - -) evolution *versus* temperature for the M_{10}-30, M_{10}-50, M_{10}-60 and M_{10}-80 membranes.

Table 5 Storage modulus of M_{10}-30, M_{10}-50, M_{10}-60 and M_{10}-80 membranes compared to the M-0 membrane (100% poly(VDF-*co*-CTFE))

	Storage modulus (Pa)				
Membrane	−50 °C	25 °C	150 °C	T_g [a] (°C)	T_g [b] (°C)
M_{10}-80	2.6×10^9	8.6×10^8	4×10^7	92.5	102
M_{10}-60	2.4×10^9	8.5×10^8	5×10^7	98	100
M_{10}-50	2.3×10^9	6.5×10^8	5×10^7	105	98
M_{10}-30	2.2×10^9	4×10^8	8×10^7	101.4	nd
M-0	2.2×10^9	3.5×10^8	2×10^8	nd	nd

[a] Determined by DSC. [b] Determined by DMA.

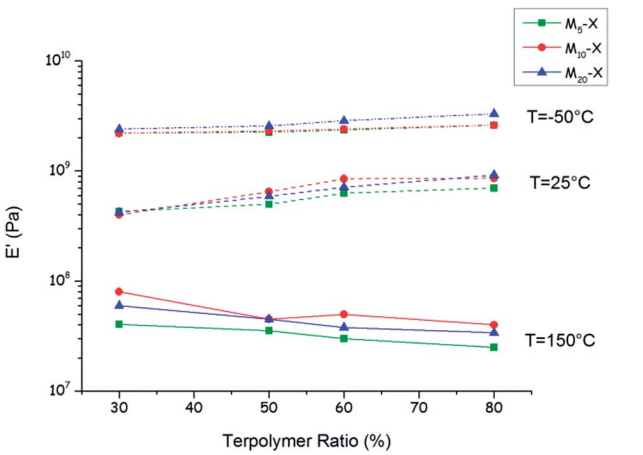

Fig. 12 Storage modulus evolution *versus* the content of phosphonate terpolymer at −50, 25 and 150 °C for the M_5-*X*, M_{10}-*X* and M_{20}-*X* membranes.

Table 6 Storage modulus evolution (in Pa) *versus* RH for the M_5-30, M_5-50, M_5-60 and M_5-80 semi-IPN membranes at RT

RH	M_5-80	M_5-60	M_5-50	M_5-30
0%	8.1×10^8	7.2×10^8	6×10^8	6.4×10^8
35%	7.1×10^8	6.4×10^8	5.2×10^8	3×10^8
70%	6.3×10^8	5.1×10^8	4.3×10^8	1.6×10^8

membranes having the highest rate of phosphonated copolymer.

In order to analyse the behaviour of the membranes in humid condition, the DMA analysis can be performed with a regulation of the RH during the analysis. To do this, the measuring chamber is crossed by the flow of neutral gas (nitrogen or argon) more or less charged with water molecules. Thus, we can observe the mechanical behaviour for RH ranging from 0 to about 80% and a temperature of 30 °C. The membranes used are very thin (about 40 μm), so it is necessary that the membranes have a significant capacity of water uptake to see an influence of RH on the mechanical behaviour. Tests conducted on the M_{20}-*X* and M_{10}-*X* membranes were not conclusive, due to too low an amount of water recovery and swelling (see Fig. 7 and 8). The most interesting results were obtained for the M_5-*X* membranes, thanks to their high values of water uptake and swelling (see Fig. 7 and 8). The results obtained are showed in Table 6.

Table 6 shows the values obtained at 0, 35 and 70% of the relative humidity for M_5-80, M_5-60, M_5-30, M_5-50 membranes. From this table, two trends are distinguishable. Indeed, when the RH is low, we can observe that a high rate of phosphonated terpolymer implies a high storage modulus. Indeed, when the RH is reduced the phosphonated terpolymer becomes more rigid, so the storage modulus is higher and the mechanical behaviour is dominated by the phosphonated terpolymer. However, at high RH, the effect is reversed. Indeed, the mechanical behaviour of the membrane is then dominated by the poly(VDF-*co*-CTFE), except for the M_5-80 membrane which possesses a high rate of phosphonated terpolymer. We find the same trend in the temperature study, *i.e.* a high rate of poly(VDF-*co*-CTFE) leads to a lower storage modulus. We can, nevertheless, conclude that, in the operating cycles of the fuel cell, the mechanical properties of membranes remain high and ensure their role as a gas barrier between two electrodes.

Experimental

Materials

Diethyl vinyl ether phosphonated was purchased from Specific Polymers (Montpellier, France). *Tert*-butylperoxypivalate (TBPPI) was kindly provided by Akzo Nobel (Compiègne, France). Chlorotrifluoroethylene (CTFE) and 1,1,1,3,3-pentafluorobutane ($C_4F_5H_5$) were kindly provided by Honeywell (Buffalo, USA) and Solvay S.A. (Tavaux, France and Bruxelles, Belgium), respectively, and were used as received. The poly(VDF-*co*-CTFE) grade was Solef 31508 supplied by Solvay. 2-Chloroethyl vinyl ether, sodium iodide, triethyl phosphite, acetone (analytical grade), methanol (analytical grade), potassium carbonate (K_2CO_3), ethyl vinyl ether, hydroxybutyl vinyl ether, mesyl chloride, triethylamine, tetrahydrofuran (THF, analytical grade), ethyl acetate (analytical grade), and hexane (analytical grade) were purchased from Sigma-Aldrich (Saint Quentin-Fallavier, France). Deuterated solvents for NMR spectroscopy were purchased from Euroiso-top (Grenoble, France) (purity >99.8%).

Synthesis of 4-(vinyloxy)butyl methanesulfonate (VBMS)

As an example, in a 250 mL single-neck round bottom flask equipped with a magnetic stirrer, one equivalent hydroxybutyl vinyl ether (10 g, 86.2 mmol), 1 equivalent of mesyl chloride were introduced (9.85 g, 86.2 mmol) and 1 equivalent of triethylamine (9.6 g, 94.9 mmol) were introduced in THF (100 mL). After 2 h, the produced salts were filtered. Two liquid/liquid (water/ethyl acetate) extractions were realized and the product was obtained in a high mass yield (80%).

Radical copolymerization of CTFE with vinyl ethers

All copolymerization reactions were carried out in a 100 mL Parr autoclave equipped with a rupture disk (3000 psi), a manometer, inlet and outlet valves and a mechanical stirrer. Prior to the reaction, potassium carbonate (3 mol%, about the overall molar amount of vinyl ether(s)) was inserted in the autoclave, which was then tightly closed and pressurized with 20 bar of nitrogen to check for eventual leaks. The autoclave was then put under vacuum (10^{-2} mbar) for 2 hours to remove oxygen. The liquid phase (*i.e.* vinyl ether(s), initiator and solvent) was introduced *via* a funnel, and CTFE was transferred by double weighing (*i.e.* the difference of weight before and after gas insertion). The reaction mixture was then stirred mechanically and progressively heated at 75 °C for 8 hours. During this step, a slight increase (*i.e.* lower than 5 bar) and decrease of pressure were observed together with a strong rise of the temperature that reached about 35 °C. After the reaction completed, the autoclave was cooled in ice and degassed to release unreacted CTFE. After opening the autoclave, the product was dissolved in acetone, concentrated with a rotary evaporator, precipitated from cold methanol and filtered. The product was then dried under vacuum (10 mbar) at 60 °C for 123 hours.

Preparation of semi-IPN membranes

A specific amount of poly(CTFE-*alt*-PEVE) was dissolved in DMSO (20–25 wt%), then poly(VDF-*co*-CTFE) powder was added into the poly(CTEF-*alt*-PEVE) solution, which was stirred for several hours at 50 °C. After the poly(VDF-*co*-CTFE) was fully dissolved, the solution was cast onto a glass plate, and then dried at 80 °C for 12 h to eliminate the solvent, then at 150 °C to perform the crosslink reaction.

To obtain the phosphonic acid groups, membranes were immerged in a concentrated HCl solution (12 N) at 90 °C for 3 days. After the reaction, membranes were washed with distilled water, and then dried under vacuum at 80 °C for one night.

Nuclear magnetic resonance

The nuclear magnetic resonance (NMR) spectra were recorded on a Bruker AC 400 instrument, using deuterated chloroform, and d_7-*N*,*N*-dimethylsulfoxide as the solvents. Chemical shifts are given in parts per million (ppm). The experimental conditions for recording ^{1}H NMR spectra were as follows: flip angle 90°, acquisition time 4.5 s, pulse delay 2 s, number of scans 128.

Thermogravimetric analyses

Thermogravimetric analyses were carried out on a TGA 51 apparatus from TA Instruments, from room temperature to 600 °C, at a heating rate of 20 °C min^{-1}, under air and nitrogen.

Differential scanning calorimetry

Differential scanning calorimetry (DSC) measurements were carried out using a Perkin-Elmer Pyris 1 apparatus. Scans were recorded at a heating/cooling rate of 20 °C min^{-1} from −100 to 150 °C. A second scan was required for the assessment of the T_g, defined as the inflection point in the heat capacity jump.

The ion exchange capacity (IEC)

The ion exchange capacity (IEC) of the different blend membranes was determined from back titration. The samples were immersed and stirred in an aqueous solution of NaOH (0.1 N, 2.5 mL) and NaCl (2 N, 50 mL). This solution was back titrated with 0.01 N HCl aqueous solution. The IEC value (meq. g^{-1}) of the blended membranes was calculated using eqn (1), where V_{eq} is the volume of 0.01 HCl aqueous solutions for the volumetric titration, [OH$^-$] the OH$^-$ concentration of the initial aqueous solution and m_d the dry weight of the membrane.

$$\mathrm{IEC}(\text{meq. g}^{-1}) = \frac{[\mathrm{OH}^-]V_{eq}}{m_d} \quad (1)$$

The IEC_{theo} was calculated by using an IEC of poly(CTFE-*alt*-VEPA) equal to 7 meq. g^{-1}. For each fluorophosphonate terpolymer, the IEC_{theo} was calculated according to eqn (2):

$$\mathrm{IEC}_{theo} = (7(1 - \tau_{CL}))\tau_{ter} \quad (2)$$

where τ_{CL} is the content of crosslinking agent VBMS into the terpolymer and τ_{ter} is the content of terpolymer in the membrane.

Water uptake and swelling measurements

Water uptake was assessed from the wet and dry states of the materials according to the following protocol: the membranes were immersed in distilled water for 24 hours and then removed. The membranes were wiped with a tissue paper, and then both the mass and thickness of the blend membranes were determined in these wet conditions. The membranes were dried at 70–80 °C for 72 h to determine the dry weight and the dry film thickness. The water uptake was determined by the following equation:

$$\text{Water uptake}(\%) = \frac{m_w - m_d}{m_d}100 \quad (3)$$

where m_w is the wet mass of the blend membranes.

The theoretical water uptake was calculated by using a WU of poly(CTFE-*alt*-VEPA) equal to 65% at 100% RH. For each fluorophosphonate terpolymer, the WU_{theo} was calculated according to the equation:

$$\mathrm{WU}_{theo} = (65(1 - \tau_{CL})\tau_{ter} \quad (4)$$

The swelling of the membranes was determined by the following equation:

$$\text{Swelling } (\%) = \frac{t_w - t_d}{t_d}100 \quad (5)$$

where t_w and t_d are the wet and dry thicknesses of the blend membranes, respectively.

Mechanical properties

Dynamic-mechanical analysis (DMA) was conducted with a METRAVIB DMA 25. Uniaxial stretching of samples was performed while heating at a rate of 2°C min^{-1} from −100 to 150 °C, keeping the frequency at 1 Hz (viscoelastic region) and a constant deformation rate. The glass transition temperature was obtained from tan δ determination. It has been shown that tan δ maximum relates much better to the value obtained by DSC.[20] Furthermore, the mechanical behaviour was studied *versus* the RH range between 0 and 100% and in the temperature range between 25 and 70 °C.

Proton conductivity

The impedance of the membranes was determined by two-point probe ac impedance spectroscopy using Mates 7260 impedance analyser. The impedance measurement was carried out at various temperatures in deionized water (relative humidity 100%). Then, the proton conductivity (σ) was obtained from the following equation:

$$\sigma = \frac{l}{RS} \quad (6)$$

where σ is the proton conductivity (S cm^{-1}), R is the ohmic resistance of the membrane sample (ohm), l is the thickness of blend membrane (cm) and S is the cross-sectional area of the membrane sample (cm^2).

Conclusion

New polymer electrolyte membranes were synthesized from a semi-IPN strategy between a crosslinkable fluorophosphonated copolymer and a commercially available fluorinated copolymer. One crucial point of interest of this work concerns the synthesis of new crosslinkable polymers by a simple heat treatment. Indeed, to the authors' knowledge, this work is the first one reporting the use of mesylate groups to form a crosslinkable polymer. More investigations are, nevertheless, required to determine the exact crosslinking mechanism.

The use of a crosslinking fluorophosphonated copolymer to cast PEMFC allows us to increase the chemical stability of the membranes *versus* acid and oxidative environments. The presence of the fluorinated copolymer allows us to obtain a material with good mechanical properties, even at a high crosslinking ratio.

However, in order to obtain membranes with high values of proton conductivity, it is necessary to use fluorophosphonated copolymer with a crosslinking rate around 5 wt%. In these conditions, the proton conductivity (10 mS cm^{-1} at 90 °C) allows us to use this material as a membrane for PEMFC.

In order to enhance the proton conductivity of these membranes, it could be interesting to perform the synthesis of the terpolymer with only 2 or 3 percent of crosslinkable monomer in the composition of the poly[(CTFE-*alt*-DEVEP)-*co*-(CTFE-*alt*-VBMS)], in order for better access to the phosphonic acid groups.

Acknowledgements

This authors wish to thank Honeywell company for providing the chlorotrifluoroethylene, Solvay Flour for the 1,1,1,3,3-pentafluorobutane and Specific Polymers for the functionalized vinyl ethers. They also wish to thanks the "Agence Nationale de la Recherche" for financially supporting this research.

References

1 M. Schuster, T. Rager, A. Noda, K. D. Kreuer and J. Maier, *Fuel Cells*, 2005, **5**, 355–365.
2 S. J. Paddison, K. D. Kreuer and J. Maier, *Phys. Chem. Chem. Phys.*, 2006, **8**, 4530–4542.
3 J. Parvole and P. Jannasch, *J. Mater. Chem.*, 2008, **18**, 5547–5556.
4 J. Parvole and P. Jannasch, *J. Mater. Chem.*, 2008, **18**, 5547–5556.
5 E. Abouzari-Lotf, H. Ghassemi, A. Shockravi, T. Zawodzinski and D. Schiraldi, *Polymer*, 2011, **52**, 4709–4717.
6 N. Y. Abu-Thabit, S. A. Ali and S. M. Javaid Zaidi, *J. Membr. Sci.*, 2010, **360**, 26–33.
7 T. Bock, H. Möhwald and R. Mülhaupt, *Macromol. Chem. Phys.*, 2007, **208**, 1324–1340.
8 B. Liu, G. P. Robertson, M. D. Guiver, Z. Shi, T. Navessin and S. Holdcroft, *Macromol. Rapid Commun.*, 2006, **27**, 1411–1417.
9 K. D. Papadimitriou, A. K. Andreopoulou and J. K. Kallitsis, *J. Polym. Sci., Part A-1: Polym. Chem.*, 2010, **48**, 2817–2827.
10 Q. Wu and R. A. Weiss, *J. Polym. Sci., Part B: Polym. Phys.*, 2004, **42**, 3628–3641.
11 Y. Tamura, L. Sheng, S. Nakazawa, T. Higashihara and M. Ueda, *J. Polym. Sci., Part A-1: Polym. Chem.*, 2012, **50**, 4334–4340.
12 R. Tayouo, G. David, B. Ameduri, S. Roualdes, H. Galiano and J. Bigarre, *France Pat.*, WO2011048076A1, 2011.
13 R. Tayouo, G. David and B. Ameduri, *Eur. Polym. J.*, 2010, **46**, 1111–1118.
14 R. Tayouo, G. David, B. Ameduri, J. Roziere and S. Roualdes, *Macromolecules*, 2010, **43**, 5269–5276.
15 B. Boutevin, F. Cersosimo and B. Youssef, *Macromolecules*, 1992, **25**, 2842–2846.
16 E. Labalme, G. David, J. Souquet-Grumey, P. Buvat and J. Bigarre, *J. Membr. Sci.*, 2014, submitted.
17 P. Buvat, J. Bigarre, J. Souquet-Grumey, G. David, E. Labalme, C. Loubat and G. Boutevin, *France Pat.*, 16 62634, 2014.
18 N. W. Sach, D. T. Richter, S. Cripps, M. Tran-Dube, H. Zhu, B. Huang, J. Cui and S. C. Sutton, *Org. Lett.*, 2012, **14**, 3886–3889.
19 G. Gebel, P. Aldebert and M. Pineri, *Polymer*, 1993, **34**, 333–339.
20 M.-I. Felisberti, L. L. de Lucca Freitas and R. Stadler, *Polymer*, 1990, **31**, 1441–1448.